

MLIP-MC: A Framework for Adsorption Simulations using Machine-Learned Interatomic Potentials

Connor W. Edwards¹, Fengxu Yang¹, Konstantin Stracke¹, and Jack D. Evans^{*1}

¹School of Physics, Chemistry and Earth Sciences, Adelaide University, North Terrace, Adelaide, 5005, South Australia, Australia

Abstract

Grand canonical Monte Carlo (GCMC) simulations are essential for screening metal–organic frameworks (MOFs) for gas adsorption, yet their accuracy is limited by underlying interatomic potentials. Universal machine-learned interatomic potentials (MLIPs), trained on diverse chemical datasets, promise zero-shot prediction without system-specific training. We introduce MLIP-MC, an open-source Python framework to conduct GCMC simulations with MLIPs, and use this framework to benchmark a series of universal models, including MACE-MP-0, ORB-v3, and fairchem ODAC, for CO₂ adsorption on ZIF-8, ZIF-4, and Mg-MOF-74. All universal models exhibit systematic biases, consistently over- or underestimating adsorption energetics. Crucially, accuracy depends on training data composition: only models trained on MOF-adsorbate interactions achieve reasonable agreement with a density functional theory derived reference. Errors grow linearly with CO₂ uptake, reflecting compounding inaccuracies in adsorbate–adsorbate interactions. Our results demonstrate that current universal MLIPs require finetuning for quantitative adsorption predictions and demonstrate the power of MLIP-MC to rapidly test models.

^{*}Corresponding author: j.evans@adelaide.edu.au

1 Introduction

Gas adsorption in porous materials underpins a diverse range of industrial processes and emerging technologies critical to modern society. Since the commercialisation of synthetic zeolites in the 1950s, adsorption-based separations have become essential to petroleum refining, air separation, and chemical processing.^[1] Metal-organic frameworks (MOFs) have emerged as a revolutionary class of porous adsorbents.^[2] Constructed from metal clusters and organic linkers, MOFs offer unprecedented tunability: in principle, an almost unlimited number of distinct frameworks can be synthesized by varying the building blocks. This structural diversity creates exciting opportunities for optimising materials for specific applications, from carbon capture and natural gas storage to drug delivery and catalysis.^[3–6]

High-throughput computational screening is a powerful research tool to address the challenge of optimising MOFs. Snurr and coworkers demonstrated that molecular simulations can rapidly evaluate the adsorption properties of thousands of MOF structures, enabling the discovery of structure–property relationships and identification of top-performing candidates prior to synthesis.^[7] The construction of computation-ready databases such as CoRE-MOF, containing over 10 000 experimentally characterized structures, has accelerated these efforts.^[8] Large-scale screening of hypothetical MOFs has revealed key structure–property relationships for methane storage and CO₂ capture.^[9] Grand Canonical Monte Carlo (GCMC) simulations, combined with classical force fields such as UFF (Universal Force Field) or DREIDING, now routinely screen databases of hypothetical and experimental MOFs.^[10] However, the accuracy of these screening studies is fundamentally limited by the underlying force fields or classical potentials. Generic potentials like UFF were parametrised for organic molecules and often fail to capture the subtle electronic effects that govern adsorption on MOFs, particularly the strong interactions at open metal sites or the cooperative binding observed in flexible frameworks.^[11] This limitation has motivated extensive efforts to develop more accurate descriptions of host-guest interactions through ab initio methods.

Sauer and coworkers have pioneered the application of high-level quantum chemical methods to achieve high accuracy (errors below 4 kJ mol^{−1}) for adsorption on zeolites and MOFs.^[12] For example, their hybrid MP2 and density functional theory (DFT) approach combines periodic DFT for the extended framework with correlated wavefunction methods (MP2, coupled cluster) for the local adsorption site, enabling quantitative prediction of adsorption enthalpies for small molecules including water, alkanes, and CO₂.^[13] These calculations have provided benchmark-quality data for understanding water-zeolite interactions,^[14] alcohol adsorption, and catalytic reaction mechanisms, while also revealing the limitations of standard DFT functionals for describing dispersion-dominated physisorption.^[12]

Despite these advances, ab initio methods remain computationally prohibitive for the extensive configurational sampling required in Monte Carlo simulations. A single DFT energy evaluation for a MOF unit cell may require minutes to hours, and GCMC simulations demand millions of energy calculations. This computational gap has limited the impact of ab initio accuracy on practical screening studies. Machine-learned interatomic potentials (MLIPs) offer a compelling solution to bridge this gap, achieving near-DFT accuracy at a fraction of the computational cost.^[15, 16] Goeminne et al. demonstrated that MLIPs trained on high-level DFT interaction energies can enable accurate GCMC simulations of MOFs, in comparison to experiment, deriving adsorption isotherms for CO₂ on both ZIF-8 and the open-metal site containing Mg-MOF-74.^[17] However, this approach requires system-specific training data for each MOF of interest.

Recent developments have produced several universal MLIPs trained on massive datasets spanning diverse chemical space.^[18] These models offer the potential for zero-shot prediction, without system-specific retraining. These include MACE-MP-0, trained on the Materials Project trajectory dataset using higher-order equivariant message passing^[19]; the Orb family of models,

employing graph network simulators optimised for inference speed[20, 21]; and the fairchem UMA models, leveraging mixture-of-linear-experts architectures to unify multiple application domains including catalysis, bulk materials, and, critically, direct air capture through the ODAC datasets.[22, 23]

In this work, we introduce MLIP-MC, an open-source Python framework that enables Monte Carlo simulations of gas adsorption using machine-learned interatomic potentials. We use this framework to systematically benchmark the leading universal MLIPs (orb-v3-conservative-informat, MACE-MP-0a, MACE-MP-0b3, MACE-MPA-0, fairchem ODAC23, fairchem ODAC25) to predict the CO₂ adsorption properties on three representative MOFs: ZIF-8, Mg-MOF-74, and ZIF-4.[24, 25] These systems were chosen to span a range of adsorption mechanisms: ZIF-8 features purely physisorptive interactions in cage-like cavities, Mg-MOF-74 exhibits strong chemisorptive binding at open metal sites, and ZIF-4 represents a dense, narrow-pore framework. We compare universal MLIP predictions against the reference finetuned model reported by Goeminne et al.,[17] trained on ab initio adsorption data, to quantify the accuracy and limitations of zero-shot prediction, and to assess whether universal MLIPs have reached sufficient maturity for practical adsorption screening applications.

2 Computational methods

2.1 MLIP-MC framework

MLIP-MC is implemented in Python and builds upon the Atomic Simulation Environment (ASE) for structure manipulation and calculator interfaces.[26] The framework currently provides two primary simulation capabilities: Widom insertion calculations for determining isosteric heats of adsorption at infinite dilution [27] and GCMC simulations for computing adsorption isotherms. Users can interact with the framework either through a robust command-line interface (`mlip_mc`) for direct shell execution or via high-level Python wrappers such as `run_gcmc()` and `run_widom()` for programmatic control and seamless integration into larger computational workflows. The GCMC implementation follows the standard Metropolis algorithm with molecule insertion, deletion, rotation, and translation moves.[28] A rejection criterion is implemented should a move cause van der Waals overlap between the adsorbate and the framework, or other adsorbates. Van der Waals radii are taken from the default ASE values and, as reported by Goeminne et al., the predicted interaction energies appear insensitive to the chosen radii.[17] This van der Waals overlap check is also applied during the attempted Widom insertion steps.

Thermodynamic consistency is maintained through the Peng-Robinson equation of state (PREOS), which computes the chemical potential and fugacity coefficients based on temperature and pressure conditions. A built-in table of critical parameters for common adsorbates is automatically applied during simulation. The MLIP-MC framework supports both equilibration phases (where configurations are sampled but not recorded) and production phases (where ensemble averages are computed).

During execution, MLIP-MC also constantly records restart data at every simulation step to ensure seamless recovery against wall-time limitations and unforeseen system interruptions. Currently, MLIP-MC supports three MLIP backends: FAIRChem for models trained within the Open Catalyst framework, MACE-Torch for MACE-architecture models and Orbital for the Orbital models.[21, 29–31] The framework was further adapted to support Nequip models, and a branch was implemented to run the finetuned models reported by Goeminne et al.[17] The model weights can be loaded from local files or automatically downloaded from Hugging Face repositories.[32] Pore size calculations were performed using ZEO++.[33]

2.2 Simulation details

Our MLIP-MC framework was used to perform Widom insertion and GCMC simulations of CO₂ on ZIF-8, Mg-MOF-74, and ZIF-4. Overall, six universal models were benchmarked against data generated using a finetuned model provided by Goeminne et al.; MACE-MP-0a,[19] MACE-MP-0b3,[19] MACE-MPA-0,[19] ORB-v3-inf-conv-omat,[21] fairchem ODAC23,[29] and fairchem ODAC25[34] (Table 1).

Table 1: Summary of universal MLIP models employed. Models are classified by architecture: Graph Neural Network (GNN), Graph Network Simulator (GNS), or Graph Transformer (GT). Training datasets and computational efficiency are also listed. Efficiency was computed on a single NVIDIA A100 GPU (SXM4, 40 GB).

Name	DOI	Class	Efficiency (s/step)	Datasets
ORB-v3-inf-conv-omat	10.48550/ARXIV.2504.06231	GNS	0.0167	OMat[35]
MACE-MP-0a	10.1063/5.0297006	GNN	0.0081	MPtrj[36]
MACE-MP-0b3	10.1063/5.0297006	GNN	0.0231	MPtrj[36]
MACE-MPA-0	10.1063/5.0297006	GNN	0.0279	MPtrj[36] + sAlex[37]
fairchem ODAC23	10.5281/zenodo.15587498	GT	0.0556	ODAC23[23]
fairchem ODAC25 (full)	10.5281/zenodo.15587498	GT	0.1431	ODAC25[34]

For the Widom insertion simulations, 100 000 insertion steps were performed with all insertion energies recorded for configurations in which the inserted CO₂ molecule did not exhibit van der Waals overlap with the framework. Each simulation then provided the average Widom insertion energy, the Boltzmann-weighted average of the insertion energy and the isosteric heat of adsorption at zero coverage. The Widom insertion energy was used to compute an isosteric heat at infinite dilution using Equation 1:

$$Q_{st,dilution} = -\frac{\langle \Delta E \exp(-\beta \Delta E) \rangle}{\langle \exp(-\beta \Delta E) \rangle} + RT, \quad (1)$$

where $\beta = (k_B T)^{-1}$, k_B is the Boltzmann constant, T is the temperature, and ΔE denotes the CO₂ insertion energy.

GCMC simulations were performed at 273 K (for ZIF-4 and ZIF-8) and 298 K (for Mg-MOF-74) for 14 pressures; 0.0002, 0.001, 0.005, 0.02, 0.05, 0.1, 0.2, 0.5, 1, 2, 5, 10, 20 and 50 bar. Each simulation comprised 100 000 equilibration steps followed by 1 000 000 production steps with an equal probability of a rotation, translation, insertion or deletion move. A van der Waals overlap check was employed to ensure the move did not cause overlap between adsorbate and framework atoms. The accepted production steps were subsequently used to calculate the isosteric heat of adsorption using Equation 2:

$$Q_{st} = -\frac{\langle EN \rangle - \langle E \rangle \langle N \rangle}{\langle N^2 \rangle - \langle N \rangle^2} + RT \quad (2)$$

where N is the number of adsorbed CO₂ molecules and E is the total interaction energy of the system. In this description, the isosteric heat captures both framework–adsorbate and adsorbate–adsorbate interactions.

3 Results and discussion

To test the MLIP-MC framework, six universal models were explored with diverse classes and training datasets (Table 1). The training datasets vary in their relevance to adsorption. MPtrj, OMat and sAlex contain DFT calculations of inorganic materials derived from the Materials Project and the Alexandria databases but include no adsorption data. The Open Direct Air

Capture datasets (ODAC23 and ODAC25) were specifically constructed to examine gas adsorption, covering single adsorption and co-adsorption of CO₂ and H₂O on MOFs. The ODAC25 dataset extends the ODAC23 to include structures with multiple adsorbate molecules, sampling higher CO₂ uptake. However, the exact distribution of adsorbed CO₂ molecules in the ODAC25 is unclear.

The reference data for GCMC simulations (uptake and isosteric heat data) were taken from results reported by Goeminne et al. using their finetuned models (model_ZIF8_N=1000.pth, model_MgMOF74_pbed3.pth, model_ZIF3_4_6_8.pth).[17] As Widom insertion results were not provided, the MLIP-MC framework was adapted to support Nquip models (molmod branch) and used to create reference isosteric heats for each MOF using these finetuned models.

3.1 Isosteric heat of adsorption at infinite dilution

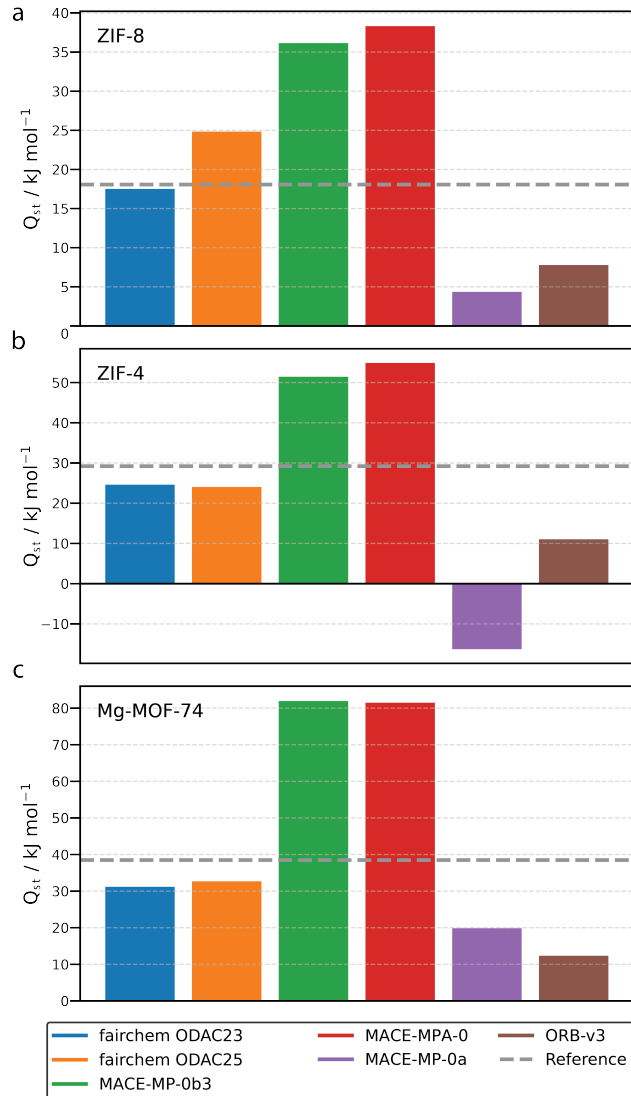


Figure 1: Isosteric heat of adsorption of CO₂ at infinite dilution ($Q_{st,dilution}$) on a) ZIF-8, b) ZIF-4 and c) Mg-MOF-74 calculated by Widom insertion for a series of universal models. Reference data from the finetuned model of Goeminne et al.[17]

The systematic trends in the isosteric heat at infinite dilution across the universal models

are illustrated in Figure 1. Rather than exhibiting framework-specific errors, the models display a systematic bias across all three MOFs, either over- or underestimating the reference isosteric heat values.

Unsurprisingly, the fairchem ODAC family of models shows the strongest overall agreement with the reference data. Both models generally underestimate the isosteric heat across all frameworks; however, the ODAC25 model slightly overestimates the predicted adsorption strength of ZIF-8, which has a large pore size and no open metal sites. In contrast, the MACE-based models exhibit large deviations from the reference. MACE-MP-0b3 and MACE-MPA-0 systematically overestimate the isosteric heat for all MOFs, with the magnitude increasing for Mg-MOF-74, containing open metal sites. This behaviour suggests a tendency of these models to exaggerate the MOF-CO₂ interaction strength. Conversely, the MACE-MP-0a model consistently underestimates the isosteric heat of adsorption, even producing negative values for ZIF-4. Given that the MACE models share similar architectures, these results underscore the significance of training data for model accuracy. Similarly, ORB-v3 consistently underestimates the isosteric heat across all frameworks.

Overall, no model achieves quantitative agreement with the reference Widom insertion results across all frameworks, though fairchem ODAC model family shows good agreement. The consistency of the observed over- and underbinding trends across the three MOFs indicates that these errors are governed by the nature and coverage of the training data rather than being a framework-dependent problem. As the ODAC/ODAC25 datasets include MOF-CO₂ interactions, predictably models trained on these data generate the best results. However, these Widom results only involve one CO₂ molecule; it is therefore important to consider how these results scale with the amount of CO₂ adsorbed.

3.2 Adsorption isotherms

Models can be generally classified into two categories: those that systematically underestimate the interaction energies (fairchem ODAC, MACE-MP-0a and ORB-v3) and those that overestimate them (MACE-MPA-0, MACE-MP-0b3). The impact of these over- and underpredictions of the isosteric heat is directly reflected in the uptake of CO₂. Models that underestimate the isosteric heat also underestimate the CO₂ uptake, as the reduced heat released upon adsorption makes the process less thermodynamically favourable. In contrast, models that overestimate the isosteric heat show higher CO₂ uptakes, reflecting an artificially increased driving force for adsorption.

The MACE models exhibit extreme systematic biases in the predicted isosteric heat across all investigated MOFs and pressures (Figure 2). Because MACE-MPA-0 and MACE-MP-0b3 significantly overestimate the isosteric heat, adsorption becomes too favourable. As a consequence, these models completely filled the pores for all MOFs, even at low pressures. Conversely, MACE-MP-0a had extremely low isosteric heats, even giving negative values for ZIF-4. This means it is thermodynamically unfavourable to adsorb CO₂, causing the pores to be empty. Increasing pressure did not significantly impact the CO₂ uptake for this model, indicating that MACE-MP-0a is unable to capture the pressure dependence of adsorption. ORB-v3 similarly underestimates the isosteric heat across all pressures, although the bias is less severe than that seen for MACE-MP-0a. Notably, none of these models are able to reproduce the distinctive pressure-dependent shape of the isosteric heat of adsorption for Mg-MOF-74, related to the filling of open metal sites.

Consistent with the Widom results, the fairchem ODAC models show a clear improvement over the MACE and ORB models, being able to approximately simulate the adsorption isotherm (Figure 3) for ZIF-4 and Mg-MOF-74 without either leaving the pore empty or completely filling the pore. While fairchem ODAC had reasonable predictions for ZIF-8 at lower pressures, it fails to capture the correct adsorption behaviour at higher pressures. This behaviour likely arises from the limitations of the ODAC23 dataset, which contains only structures with up to one adsorbed

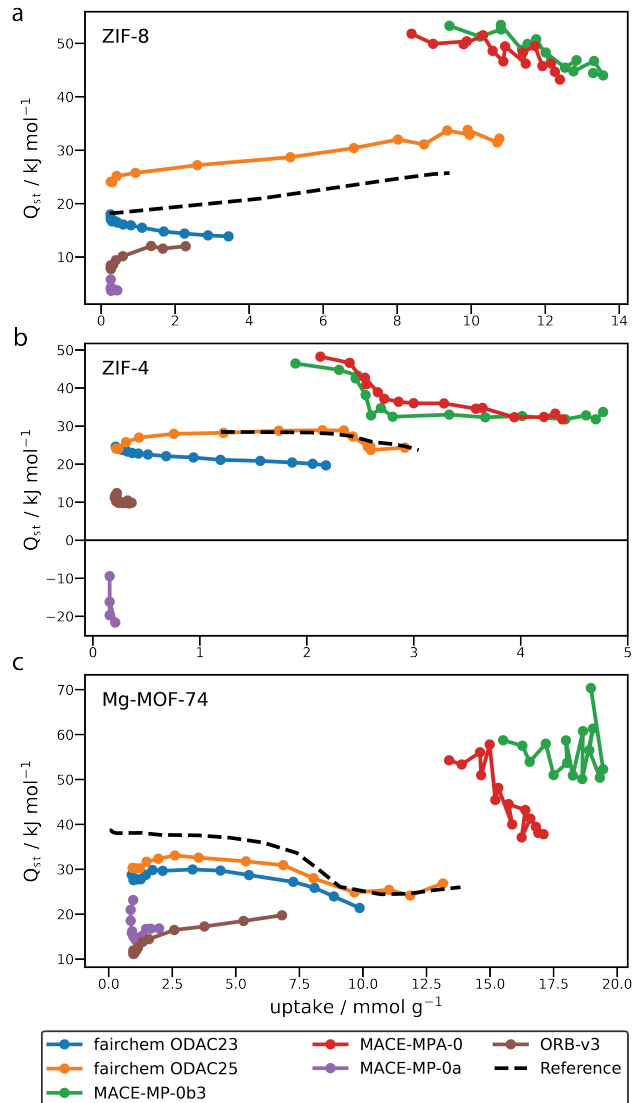


Figure 2: Isosteric heat of adsorption (Q_{st}) for CO_2 on a) ZIF-8, b) ZIF-4 and c) Mg-MOF-74 computed by GCMC simulations for a series of universal models. Reference data from a finetuned model of Goeminne et al.[17]

CO_2 molecule. As a result, the model underestimates CO_2 – CO_2 interactions and is not able to treat higher uptakes. Of the models evaluated, only the fairchem ODAC25 model is able to reproduce all key features of the reference data for ZIF-4 and Mg-MOF-74. However, fairchem ODAC25 fails to quantitatively describe ZIF-8, systematically overestimating the isosteric heat of adsorption.

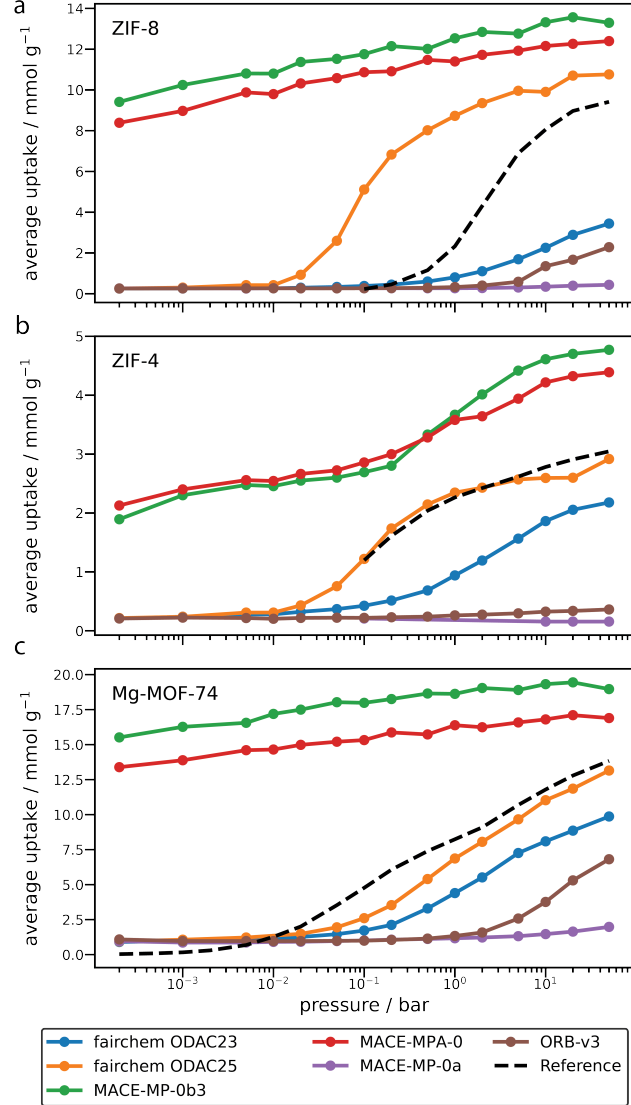


Figure 3: CO_2 adsorption isotherms for a) ZIF-8, b) ZIF-4 and c) Mg-MOF-74 calculated using GCMC simulations for a series of universal models. Reference data from the finetuned model of Goeminne et al.[17]

This discrepancy likely arises from an inaccurate representation of framework– CO_2 interactions. Although ZIF-8 and Mg-MOF-74 have comparable pore sizes, 11.8 Å and 11.7 Å respectively (computed by ZEO++), their adsorption mechanisms differ substantially. Mg-MOF-74 contains open metal sites that strongly bind CO_2 . This leads to a high isosteric heat at low pressures, which decreases as these sites become saturated. In contrast, ZIF-8 lacks open metal sites and adsorption is dominated by weaker dispersive interactions. Consequently, ZIF-8 is expected to exhibit lower isosteric heat than Mg-MOF-74, as reflected in the reference data and fairchem ODAC25 results. However, fairchem ODAC25 systematically overestimates the isosteric heat

of adsorption for ZIF-8 across all pressures, suggesting the model overemphasises pore size as a driving factor for adsorption. For Mg-MOF-74, the isosteric heat is underestimated at lower uptakes, suggesting the binding strength to open metal sites is underestimated. As pressure and CO₂ uptake increase, these open metal sites become saturated and CO₂ starts filling the pore (Supplementary Figure 1). As this happens, the model more closely reproduces the reference behaviour. While this apparent agreement at higher uptakes is encouraging, it likely arises from partial error cancellation between underestimated metal–CO₂ interactions and overestimated CO₂–CO₂ interactions within the large pore. This behaviour highlights that fairchem ODAC25 does not yet robustly capture the distinct physical adsorption mechanisms governing these two frameworks.

Overall, no single model provides universally accurate adsorption energetics across all regimes. The ability to recreate the reference data is governed primarily by the training data describing CO₂–framework interactions rather than by architectural complexity. Training on datasets with multiple adsorbates such as ODAC25 showed improvements over datasets with just a single adsorbate such as ODAC23. This enables models to better describe CO₂–CO₂ interactions and give a more reliable description of the adsorption behaviour. From the models evaluated here, fairchem ODAC25 demonstrates the most reliable and transferable behaviour for predicting both adsorption energetics and CO₂ uptake, yet falls short for ZIF-8.

3.3 Shortcomings of universal models

The work so far establishes that select universal models can capture realistic isosteric heats at infinite dilution; however, only fairchem ODAC25 can recreate the work conducted by Goeminne et al.[17] for ZIF-4 and Mg-MOF-74, but not ZIF-8. To further investigate where this discrepancy arises, the ZIF-8 DFT reference data reported by Goeminne et al. (employed to train the ZIF-8 finetuned model) was used to validate the universal models and the finetuned model (Figure 4). This dataset consists of 30 000 ZIF-8 structures with CO₂ uptakes ranging from 0 to 32 molecules and between 551 and 3663 structures per uptake.

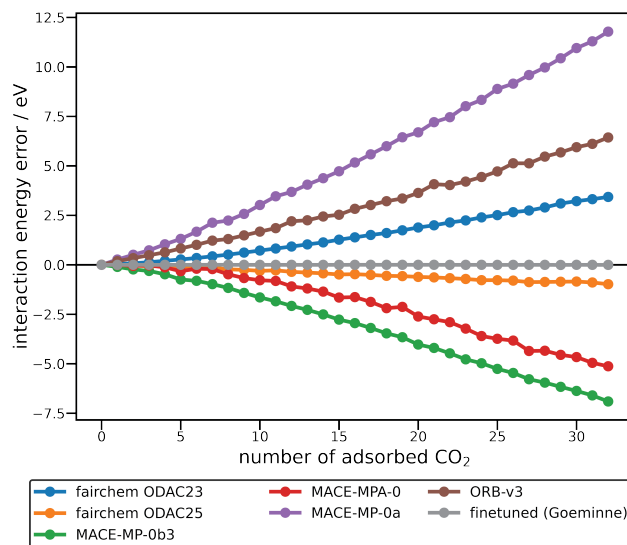


Figure 4: Error in interaction energy, model predicted relative to the reference DFT reported by Goeminne et al.[17], with increasing CO₂ molecules for the adsorption on ZIF-8.

As expected, the model finetuned on this dataset reproduced the DFT interaction energies across all uptakes. In contrast, the universal models all exhibited uptake-dependent error.

While their performance is reasonable at low uptake, the error in interaction energy grows approximately linearly with increasing CO_2 uptake. Consistent with the Widom and GCMC simulations, MACE-MP-0a, ORB-v3 and fairchem ODAC overestimate the interaction energies and MACE-MPA-0, MACE-MP-0b3 underestimate the insertion energies. Fairchem ODAC25 performs significantly better than other universal models across all uptakes. However, fairchem ODAC25 still slightly underestimates the interaction energy.

The near linear growth in interaction error suggests the accuracy of these models has a strong dependence on the CO_2 uptake. At low uptakes, the level of error is dependent on the ability of the model to describe framework- CO_2 interactions. As the uptake increases, CO_2 - CO_2 interactions become more prevalent and have a larger contribution to the total error. The linear trend indicates that both interaction regimes are described with comparable inaccuracy. There is a subtle increase in error around 8 CO_2 molecules (most noticeable in MACE-MPA-0) which corresponds to when CO_2 - CO_2 interactions begin to dominate. This suggests that overall CO_2 - CO_2 interactions are represented less accurately than framework- CO_2 interactions.

CO_2 interaction error becomes more evident when considering the error per CO_2 , which retains a linear increase for most models (Supplementary Figure 2). As the number of CO_2 molecules grows, so too does the number of CO_2 - CO_2 interactions, leading to compounding errors. Notably, fairchem ODAC25 exhibits a flat error per CO_2 profile, suggesting a systematic offset in CO_2 - CO_2 interactions rather than the loading-dependent errors seen in the other models. This improved behaviour arises from its training dataset, which includes structures with multiple adsorbates, enabling a more accurate representation of intermolecular interactions at higher uptakes. However, even fairchem ODAC25 fails to quantitatively reproduce reference interaction energies, highlighting the need for system-specific finetuned models.

Beyond accuracy, the fastest universal model evaluated (MACE-MP-0a) demonstrates comparable computational efficiency to the finetuned Mg-MOF-74 model. In contrast, both fairchem models are significantly less efficient than the other universal models, with the ODAC25 model being 14 times slower than the finetuned model. As a result, even though fairchem ODAC25 was the only universal model to reproduce isotherm behaviours, the high computational cost limits its practicality for longer simulations or extensive high-pressure screening studies. This further highlights the importance of developing finetuned models that can achieve both accuracy and computational efficiency.

The efficiency metrics reported in Table 1 should be treated with caution, as efficiency will depend on the amount of adsorbed CO_2 . Models that predict little to no uptake, such as MACE-MP-0a, will appear artificially more efficient than models that predict higher uptakes. Because the number of atoms varies during the simulation, these efficiencies have not been normalised on a per-atom basis. Instead, they reflect the real-world production efficiency of applying each model to Mg-MOF-74 at 1 bar and 273 K.

4 Summary and Outlook

In this work, we introduced MLIP-MC, an open-source Python framework that enables Widom insertions and GCMC simulations using universal MLIPs. We benchmarked six universal models against a reference dataset obtained from a series of finetuned models trained for CO_2 adsorption on ZIF-8, ZIF-4 and Mg-MOF-74.

Across Widom and GCMC simulations, all MLIPs exhibited systematic biases in their interaction energies. Rather than being system-specific, these biases resulted from the models under- or overestimating the CO_2 interaction energies. Consequently, MACE-MPA-0 and MACE-MP-0b3 artificially filled the available pores, while MACE-MP-0a, ORB-v3 and fairchem ODAC produced partially or fully empty pores across all pressures. Of the models evaluated, only fairchem ODAC25 showed reliable results, successfully reproducing the reference isotherms for ZIF-4 and Mg-MOF-74. However, fairchem ODAC25 was unable to properly describe CO_2 up-

take in ZIF-8 due to overemphasising the role of CO₂-CO₂ interactions, and thus pore size, in the absence of open metal sites. Additionally, the computational inefficiency of the fairchem ODAC models limits their practical applicability.

These results demonstrate that existing universal MLIPs are unable to reliably describe gas adsorption across diverse systems and that finetuned models are required to capture the correct thermodynamic behaviour of adsorbed gases. Incorporating more adsorption structures in training datasets and extending these to cover systems beyond one adsorbed CO₂, such as ODAC25, significantly improves the accuracy of these models. This highlights the importance of high-quality and diverse training data for future MLIPs. The MLIP-MC framework enables benchmarking and the deployment and training of new MLIPs. We expect the next generation of accurate and efficient models will enable high-throughput discovery and screening of new porous materials using MLIPs for gas separation and storage applications.

Supporting Information

MLIP-MC is available on GitHub . All code and data for this research are available on Zenodo: [10.5281/zenodo.18637262](https://doi.org/10.5281/zenodo.18637262). Figures of the CO₂ distribution on Mg-MOF-74 and error analysis are provided in the Supplementary Information.

Acknowledgements

J.D.E. is the recipient of an Australian Research Council Discovery Early Career Award (project number DE220100163) funded by the Australian Government. Phoenix HPC service at Adelaide University is thanked for providing high-performance computing resources. This research was supported by the Australian Government's National Collaborative Research Infrastructure Strategy (NCRIS), with access to computational resources provided by Pawsey Supercomputing Research Centre through the National Computational Merit Allocation Scheme.

References

- [1] Michiel Dusselier and Mark E. Davis. Small-pore zeolites: Synthesis and catalysis. *Chemical Reviews*, 118(11):5265–5329, May 2018. ISSN 1520-6890. doi: [10.1021/acs.chemrev.7b00738](https://doi.org/10.1021/acs.chemrev.7b00738). URL <http://dx.doi.org/10.1021/acs.chemrev.7b00738>.
- [2] Hiroyasu Furukawa, Kyle E. Cordova, Michael O’Keeffe, and Omar M. Yaghi. The chemistry and applications of metal-organic frameworks. *Science*, 341(6149), August 2013. ISSN 1095-9203. doi: [10.1126/science.1230444](https://doi.org/10.1126/science.1230444). URL <http://dx.doi.org/10.1126/science.1230444>.
- [3] Shreya Mahajan and Manu Lahtinen. Recent progress in metal-organic frameworks (mofs) for co2 capture at different pressures. *Journal of Environmental Chemical Engineering*, 10(6):108930, December 2022. ISSN 2213-3437. doi: [10.1016/j.jece.2022.108930](https://doi.org/10.1016/j.jece.2022.108930). URL <http://dx.doi.org/10.1016/j.jece.2022.108930>.
- [4] Karabi Nath, Keenan R. Wright, Alauddin Ahmed, Donald J. Siegel, and Adam J. Matzger. Adsorption of natural gas in metal-organic frameworks: Selectivity, cyclability, and comparison to methane adsorption. *Journal of the American Chemical Society*, 146(15):10517–10523, April 2024. ISSN 1520-5126. doi: [10.1021/jacs.3c14535](https://doi.org/10.1021/jacs.3c14535). URL <http://dx.doi.org/10.1021/jacs.3c14535>.
- [5] Isabel Abánades Lázaro, Connor J. R. Wells, and Ross S. Forgan. Multivariate modulation of the zr mof uiio-66 for defect-controlled combination anticancer drug delivery. *Angewandte*

Chemie International Edition, 59(13):5211–5217, February 2020. ISSN 1521-3773. doi: 10.1002/anie.201915848. URL <http://dx.doi.org/10.1002/anie.201915848>.

- [6] Oliver M. Linder-Patton, Lizhuo Wang, Jack D. Evans, Nor Hafizah Yasin, Nor Hafizah Berahim-Jusoh, Siqi Li, Jun Huang, Chan Zhe Phak, Akbar A. Seman, Christopher J. Sumby, and Christian J. Doonan. Understanding the role of the zr-mof support structure on templated ternary co 2 hydrogenation catalyst structure and activity. *ACS Applied Materials & Interfaces*, 17(31):44573–44584, July 2025. ISSN 1944-8252. doi: 10.1021/acsami.5c10085. URL <http://dx.doi.org/10.1021/acsami.5c10085>.
- [7] Yamil J. Colón and Randall Q. Snurr. High-throughput computational screening of metal–organic frameworks. *Chem. Soc. Rev.*, 43(16):5735–5749, 2014. ISSN 1460-4744. doi: 10.1039/c4cs00070f. URL <http://dx.doi.org/10.1039/c4cs00070f>.
- [8] Yongchul G. Chung, Jeffrey Camp, Maciej Haranczyk, Benjamin J. Sikora, Wojciech Bury, Vaiva Krungleviciute, Taner Yildirim, Omar K. Farha, David S. Sholl, and Randall Q. Snurr. Computation-ready, experimental metal–organic frameworks: A tool to enable high-throughput screening of nanoporous crystals. *Chemistry of Materials*, 26(21):6185–6192, October 2014. ISSN 1520-5002. doi: 10.1021/cm502594j. URL <http://dx.doi.org/10.1021/cm502594j>.
- [9] Christopher E. Wilmer, Michael Leaf, Chang Yeon Lee, Omar K. Farha, Brad G. Hauser, Joseph T. Hupp, and Randall Q. Snurr. Large-scale screening of hypothetical metal–organic frameworks. *Nature Chemistry*, 4(2):83–89, November 2011. ISSN 1755-4349. doi: 10.1038/nchem.1192. URL <http://dx.doi.org/10.1038/nchem.1192>.
- [10] David Dubbeldam, Sofía Calero, Donald E. Ellis, and Randall Q. Snurr. Raspa: molecular simulation software for adsorption and diffusion in flexible nanoporous materials. *Molecular Simulation*, 42(2):81–101, February 2015. ISSN 1029-0435. doi: 10.1080/08927022.2015.1010082. URL <http://dx.doi.org/10.1080/08927022.2015.1010082>.
- [11] A. K. Rappe, C. J. Casewit, K. S. Colwell, W. A. Goddard, and W. M. Skiff. Uff, a full periodic table force field for molecular mechanics and molecular dynamics simulations. *Journal of the American Chemical Society*, 114(25):10024–10035, December 1992. ISSN 1520-5126. doi: 10.1021/ja00051a040. URL <http://dx.doi.org/10.1021/ja00051a040>.
- [12] Joachim Sauer. Ab initio calculations for molecule–surface interactions with chemical accuracy. *Accounts of Chemical Research*, 52(12):3502–3510, November 2019. ISSN 1520-4898. doi: 10.1021/acs.accounts.9b00506. URL <http://dx.doi.org/10.1021/acs.accounts.9b00506>.
- [13] GiovanniMaria Piccini, Maristella Alessio, Joachim Sauer, Yuchun Zhi, Yuanshuai Liu, Robin Kolvenbach, Andreas Jentys, and Johannes A. Lercher. Accurate adsorption thermodynamics of small alkanes in zeolites. ab initio theory and experiment for h-chabazite. *The Journal of Physical Chemistry C*, 119(11):6128–6137, March 2015. ISSN 1932-7455. doi: 10.1021/acs.jpcc.5b01739. URL <http://dx.doi.org/10.1021/acs.jpcc.5b01739>.
- [14] Katarina Stanciakova, Jaap N. Louwen, Bert M. Weckhuysen, Rosa E. Bulo, and Florian Görtl. Understanding water–zeolite interactions: On the accuracy of density functionals. *The Journal of Physical Chemistry C*, 125(37):20261–20274, September 2021. ISSN 1932-7455. doi: 10.1021/acs.jpcc.1c04270. URL <http://dx.doi.org/10.1021/acs.jpcc.1c04270>.
- [15] Connor W. Edwards, Oliver M. Linder-Patton, and Jack D. Evans. Simulations of high temperature decomposition of metal-organic frameworks to form amorphous catalysts, 2026. URL <https://arxiv.org/abs/2601.16459>.

- [16] Connor W. Edwards and Jack D. Evans. Exploring foundational machine learned potentials for treating the high temperature dynamics of metal-organic frameworks. *Advanced Theory and Simulations*, 9(2), October 2025. ISSN 2513-0390. doi: 10.1002/adts.202500514. URL <http://dx.doi.org/10.1002/adts.202500514>.
- [17] Ruben Goeminne, Louis Vanduyfhuys, Veronique Van Speybroeck, and Toon Verstraelen. Dft-quality adsorption simulations in metal-organic frameworks enabled by machine learning potentials. *Journal of Chemical Theory and Computation*, 19(18):6313–6325, August 2023. ISSN 1549-9626. doi: 10.1021/acs.jctc.3c00495. URL <http://dx.doi.org/10.1021/acs.jctc.3c00495>.
- [18] Bowen Deng, Yunyeong Choi, Peichen Zhong, Janosh Riebesell, Shashwat Anand, Zhuohan Li, KyuJung Jun, Kristin A. Persson, and Gerbrand Ceder. Systematic softening in universal machine learning interatomic potentials. *npj Computational Materials*, 11(1), January 2025. ISSN 2057-3960. doi: 10.1038/s41524-024-01500-6. URL <http://dx.doi.org/10.1038/s41524-024-01500-6>.
- [19] Ilyes Batatia, Philipp Benner, Yuan Chiang, Alin M. Elena, Dávid P. Kovács, Janosh Riebesell, Xavier R. Advincula, Mark Asta, Matthew Avaylon, William J. Baldwin, Fabian Berger, Noam Bernstein, Arghya Bhowmik, Filippo Bigi, Samuel M. Blau, Vlad Cărare, Michele Ceriotti, Sanggyu Chong, James P. Darby, Sandip De, Flaviano Della Pia, Volker L. Deringer, Rokas Elijošius, Zakariya El-Machachi, Edvin Fako, Fabio Falcioni, Andrea C. Ferrari, John L. A. Gardner, Mikołaj J. Gawkowski, Annalena Genreith-Schriever, Janine George, Rhys E. A. Goodall, Jonas Grandel, Clare P. Grey, Petr Grigorev, Shuang Han, Will Handley, Hendrik H. Heenen, Kersti Hermansson, Cheuk Hin Ho, Stephan Hofmann, Christian Holm, Jad Jaafar, Konstantin S. Jakob, Hyunwook Jung, Venkat Kapil, Aaron D. Kaplan, Nima Karimitari, James R. Kermode, Panagiotis Kourtis, Namu Kroupa, Jolla Kullgren, Matthew C. Kuner, Domantas Kuryla, Guoda Liepuoniute, Chen Lin, Johannes T. Margraf, Ioan-Bogdan Magdău, Angelos Michaelides, J. Harry Moore, Aakash A. Naik, Samuel P. Niblett, Sam Walton Norwood, Niamh O’Neill, Christoph Ortner, Kristin A. Persson, Karsten Reuter, Andrew S. Rosen, Louise A. M. Rosset, Lars L. Schaa, Christoph Schran, Benjamin X. Shi, Eric Sivonxay, Tamás K. Stenczel, Christopher Sutton, Viktor Svahn, Thomas D. Swinburne, Jules Tilly, Cas van der Oord, Santiago Vargas, Eszter Varga-Umbrich, Tejs Vegge, Martin Vondrák, Yangshuai Wang, William C. Witt, Thomas Wolf, Fabian Zills, and Gábor Csányi. A foundation model for atomistic materials chemistry. *The Journal of Chemical Physics*, 163(18), November 2025. ISSN 1089-7690. doi: 10.1063/5.0297006. URL <http://dx.doi.org/10.1063/5.0297006>.
- [20] Mark Neumann, James Gin, Benjamin Rhodes, Steven Bennett, Zhiyi Li, Hitarth Choubisa, Arthur Hussey, and Jonathan Godwin. Orb: A fast, scalable neural network potential, 2024. URL <https://arxiv.org/abs/2410.22570>.
- [21] Benjamin Rhodes, Sander Vandenhaute, Vaidotas Šimkus, James Gin, Jonathan Godwin, Tim Duignan, and Mark Neumann. Orb-v3: atomistic simulation at scale, 2025. URL <https://arxiv.org/abs/2504.06231>.
- [22] Muhammed Shuaibi, Abhishek Das, Anuroop Sriram, Misko, Luis Barroso-Luque, Ray Gao, Siddharth Goyal, Zachary Ulissi, Brandon Wood, Tian Xie, Junwoong Yoon, Brook Wander, Adeesh Kolluru, Richard Barnes, Ethan Sunshine, Kevin Tran, Xiang, Daniel Levine, Nima Shoghi, Ilias Chair, , Janice Lan, Kaylee Tian, Joseph Musielewicz, clz55, Weihua Hu, , Kyle Michel, willis, and vbtchr. FAIRChem. URL <https://github.com/facebookresearch/fairchem>.

[23] Anuroop Sriram, Sihoon Choi, Xiaohan Yu, Logan M. Brabson, Abhishek Das, Zachary Ulissi, Matt Uyttendaele, Andrew J. Medford, and David S. Sholl. The open dac 2023 dataset and challenges for sorbent discovery in direct air capture. *ACS Central Science*, 10(5):923–941, May 2024. ISSN 2374-7951. doi: 10.1021/acscentsci.3c01629. URL <http://dx.doi.org/10.1021/acscentsci.3c01629>.

[24] Kyo Sung Park, Zheng Ni, Adrien P. Côté, Jae Yong Choi, Rudan Huang, Fernando J. Uribe-Romo, Hee K. Chae, Michael O’Keeffe, and Omar M. Yaghi. Exceptional chemical and thermal stability of zeolitic imidazolate frameworks. *Proceedings of the National Academy of Sciences*, 103(27):10186–10191, July 2006. ISSN 1091-6490. doi: 10.1073/pnas.0602439103. URL <http://dx.doi.org/10.1073/pnas.0602439103>.

[25] Rahul Banerjee, Hiroyasu Furukawa, David Britt, Carolyn Knobler, Michael O’Keeffe, and Omar M. Yaghi. Control of pore size and functionality in isoreticular zeolitic imidazolate frameworks and their carbon dioxide selective capture properties. *Journal of the American Chemical Society*, 131(11):3875–3877, March 2009. ISSN 1520-5126. doi: 10.1021/ja809459e. URL <http://dx.doi.org/10.1021/ja809459e>.

[26] Ask Hjorth Larsen, Jens Jørgen Mortensen, Jakob Blomqvist, Ivano E Castelli, Rune Christensen, Marcin Dułak, Jesper Friis, Michael N Groves, Bjørk Hammer, Cory Hargus, Eric D Hermes, Paul C Jennings, Peter Bjerre Jensen, James Kermode, John R Kitchin, Esben Leonhard Kolsbjerg, Joseph Kubal, Kristen Kaasbjerg, Steen Lysgaard, Jón Bergmann Maronsson, Tristan Maxson, Thomas Olsen, Lars Pastewka, Andrew Peterson, Carsten Rostgaard, Jakob Schiøtz, Ole Schütt, Mikkel Strange, Kristian S Thygesen, Tejs Vegge, Lasse Vilhelmsen, Michael Walter, Zhenhua Zeng, and Karsten W Jacobsen. The atomic simulation environment—a python library for working with atoms. *Journal of Physics: Condensed Matter*, 29(27):273002, June 2017. ISSN 1361-648X. doi: 10.1088/1361-648x/aa680e. URL <http://dx.doi.org/10.1088/1361-648X/aa680e>.

[27] B. Widom. Some topics in the theory of fluids. *The Journal of Chemical Physics*, 39(11):2808–2812, December 1963. ISSN 1089-7690. doi: 10.1063/1.1734110. URL <http://dx.doi.org/10.1063/1.1734110>.

[28] Daan Frenkel and Berend Smit. *Understanding Molecular Simulation: From Algorithms to Applications*. Academic Press, San Diego, CA, USA, 2 edition, 2002. ISBN 978-0122673511.

[29] facebookresearch. Fairchem: Fair chemistry’s library of machine learning methods for chemistry. <https://github.com/facebookresearch/fairchem>, 2025.

[30] Ilyes Batatia, David Peter Kovacs, Gregor N. C. Simm, Christoph Ortner, and Gabor Csanyi. MACE: Higher order equivariant message passing neural networks for fast and accurate force fields. In Alice H. Oh, Alekh Agarwal, Danielle Belgrave, and Kyunghyun Cho, editors, *Advances in Neural Information Processing Systems*, 2022. URL <https://openreview.net/forum?id=YPpSngE-ZU>.

[31] Ilyes Batatia, Simon Batzner, Dávid Péter Kovács, Albert Musaelian, Gregor N. C. Simm, Ralf Drautz, Christoph Ortner, Boris Kozinsky, and Gábor Csányi. The design space of e(3)-equivariant atom-centered interatomic potentials, 2022.

[32] Hugging Face, Inc. Hugging Face. <https://huggingface.co>, 2026. Accessed: 2026-02-12.

[33] Thomas F. Willems, Chris H. Rycroft, Michaeel Kazi, Juan C. Meza, and Maciej Haranczyk. Algorithms and tools for high-throughput geometry-based analysis of crystalline porous materials. *Microporous and Mesoporous Materials*, 149(1):134–141, February 2012. ISSN 1387-1811. doi: 10.1016/j.micromeso.2011.08.020. URL <http://dx.doi.org/10.1016/j.micromeso.2011.08.020>.

- [34] Anuroop Sriram, Logan M. Brabson, Xiaohan Yu, Sihoon Choi, Kareem Abdelmaqsoud, Elias Moubarak, Pim de Haan, Sindy Löwe, Johann Brehmer, John R. Kitchin, Max Welling, C. Lawrence Zitnick, Zachary Ulissi, Andrew J. Medford, and David S. Sholl. The open dac 2025 dataset for sorbent discovery in direct air capture, 2025. URL <https://arxiv.org/abs/2508.03162>.
- [35] Luis Barroso-Luque, Muhammed Shuaibi, Xiang Fu, Brandon M. Wood, Misko Dzamba, Meng Gao, Ammar Rizvi, C. Lawrence Zitnick, and Zachary W. Ulissi. Open materials 2024 (omat24) inorganic materials dataset and models. doi: 10.48550/arXiv.2410.12771. URL <http://arxiv.org/abs/2410.12771>.
- [36] Materials Project Trajectory (MPtrj) dataset. https://figshare.com/articles/dataset/Materials_Project_Trajectory_MPtrj_Dataset/23713842, 2023. Figshare dataset (MPtrj) — accessed 2025-10-30.
- [37] sAlex: a Matbench-Discovery compliant subsample of the Alexandria dataset. <https://matbench-discovery.materialsproject.org/data/salex>, 2024. sAlex dataset used in MACE second-generation models. Accessed 2025-10-30.